The American Journal of Pathology, Vol. 186, No. 12, December 2016

ELSEVIER

The American Journal of
PATHOLOGY
ajp.amjpathol.org

MOLECULAR PATHOGENESIS OF GENETIC AND INHERITED DISEASES

BGP-15 Improves Aspects of the Dystrophic Pathology in *mdx* and *dko* Mice with Differing Efficacies in Heart and Skeletal Muscle

Tahnee L. Kennedy,* Kristy Swiderski,* Kate T. Murphy,* Stefan M. Gehrig,* Claire L. Curl,† Chanchal Chandramouli,† Mark A. Febbraio,‡ Lea M.D. Delbridge,† René Koopman,* and Gordon S. Lynch*

From the Basic and Clinical Myology Laboratory and the Cardiac Phenomics Laboratory,† Department of Physiology, The University of Melbourne, Melbourne, Victoria; and the Baker IDI Heart and Diabetes Institute,‡ Melbourne, Victoria, Australia*

Accepted for publication August 17, 2016.

Address correspondence to Gordon S. Lynch, Ph.D., Basic and Clinical Myology Laboratory, Department of Physiology, The University of Melbourne, Melbourne, VIC 3010, Australia. E-mail: gsl@unimelb.edu.au.

Duchenne muscular dystrophy is a severe and progressive striated muscle wasting disorder that leads to premature death from respiratory and/or cardiac failure. We have previously shown that treatment of young dystrophic *mdx* and dystrophin/utrophin null (*dko*) mice with BGP-15, a coinducer of heat shock protein 72, ameliorated the dystrophic pathology. We therefore tested the hypothesis that later-stage BGP-15 treatment would similarly benefit older *mdx* and *dko* mice when the dystrophic pathology was already well established. Later stage treatment of *mdx* or *dko* mice with BGP-15 did not improve maximal force of tibialis anterior (TA) muscles (*in situ*) or diaphragm muscle strips (*in vitro*). However, collagen deposition (fibrosis) was reduced in TA muscles of BGP-15—treated *dko* mice but unchanged in TA muscles of treated *mdx* mice and diaphragm of treated *mdx* and *dko* mice. We also examined whether BGP-15 treatment could ameliorate aspects of the cardiac pathology, and in young *dko* mice it reduced collagen deposition and improved both membrane integrity and systolic function. These results confirm BGP-15's ability to improve aspects of the dystrophic pathology but with differing efficacies in heart and skeletal muscles at different stages of the disease progression. These findings support a role for BGP-15 among a suite of pharmacological therapies for Duchenne muscular dystrophy and related disorders. *(Am J Pathol 2016, 186: 3246—3260; http://dx.doi.org/10.1016/j.ajpath.2016.08.008)*

Duchenne muscular dystrophy (DMD) is a severe and progressive muscle wasting disorder caused by mutations in the dystrophin gene, resulting in the absence of the membrane-stabilizing protein, dystrophin.[1,2] DMD affects approximately 1 in 3500 to 6000 live male births,[3] with patients becoming wheelchair dependent usually before their teenage years and eventually succumbing to respiratory and/or cardiac failure.[1,4,5] Although a cure for DMD will eventually come from corrective gene therapy, limitations of delivery systems, gene-carrying capacity, dissemination efficiency, expression persistence, and immunological tolerance pose significant challenges for immediate clinical application.[6]

The heat shock protein (Hsp) family is a group of proteins induced by cellular stress that are implicated in cellular protection.[7] During periods of stress, Hsp family members bind denatured proteins, preventing further breakdown and protein aggregation.[8,9] Hsp70/72 is the most widely studied and well-characterized member of the Hsp family, and its induction shown beneficial for several muscle conditions.[10—13] Up-regulation of the inducible form (Hsp72), through transgenic and pharmacological approaches, enhanced muscle strength and improved histopathological

Supported by the Muscular Dystrophy Association USA research grant MDA255253 (G.S.L.) and the National Health and Medical Research Council of Australia (NHMRC) research grant APP106546 (G.S.L.); the Heart Foundation (Australia) initially by an Australian Postgraduate Award (T.L.K.) and then a Postgraduate Scholarship (T.L.K.); NHMRC Early Career Fellowship (K.S.); NHMRC Career Development Fellowship (K.T.M.); and NHMRC Senior Principal Research Fellowship (M.A.F.).

Disclosures: BGP-15 was obtained from N-Gene Research Laboratories Inc. (United States). M.A.F. is a shareholder and Chief Scientific Officer and G.S.L. is a shareholder and consultant for this company.

Current address of M.A.F., Garvan Institute of Medical Research, Darlinghurst, NSW, Australia.

http://dx.doi.org/10.1016/j.ajpath.2016.08.008

features in the severely affected diaphragm muscles of young dystrophic *mdx* and dystrophin/utrophin double-knockout (*dko*) mice.[14] Most important for clinical application, Hsp72 induction reduced kyphosis and increased lifespan of *dko* mice.[14] BGP-15 is a pharmacological coinducer of Hsp72, shown safe and well tolerated in phase 2 clinical trials for diabetes and insulin resistance.[15,16] BGP-15 is a hydroxylamine derivative that amplifies the endogenous stress response by altering the organization of cholesterol-rich membrane domains to specifically target stressed cells.[17–20] This is a desirable trait for therapeutics administered systemically and chronically.

We investigated the effect of BGP-15 administration to young (3- to 4-week-old) *mdx* and *dko* mice and showed a dramatically improved pathophysiology and lifespan.[14] However, although DMD is diagnosed early in life, significant muscle damage will have already occurred to cause functional deficits. Early-stage treatment of *dko* mice does not correlate with the pathology of DMD patients at the time of diagnosis and so the clinical translation of these potentially beneficial effects may not be realized. This is a limitation for other potential treatments for DMD, including growth-promoting agents like myostatin inhibitory antibodies, which were beneficial only when administered early in the disease progression but not later.[21] In addition, it is unclear whether BGP-15 is similarly effective only as a preventive intervention or whether it can improve an advanced pathology. Therefore, to fully elucidate the therapeutic potential of BGP-15 for treating muscular dystrophy, we investigated whether BGP-15 treatment was similarly beneficial in older *mdx* and *dko* mice with an established pathology.

Cardiomyopathy develops throughout adolescence and is evident in most DMD patients by 18 years of age.[22] Because of improved clinical management of respiratory symptoms, cardiac problems have become a critical aspect of the disease.[23,24] Targeting only the skeletal musculature can exacerbate cardiomyopathy in *mdx* mice, suggesting increased movement and skeletal muscle activity may cause stress to the myocardium and accelerate cardiac damage.[25] In addition, long-term treatment with the tumor necrosis factor-α blocking drug infliximab (Remicade), which can benefit the skeletal muscle pathology, had significant negative effects on cardiac function in *mdx* mice.[26] These findings indicate that treating both skeletal and cardiac muscle pathology is necessary for DMD. Cardiac dysfunction is evident in dystrophic *mdx* and *dko* mice, but its severity in *dko* mice more closely resembles that in DMD.[27] Therefore, therapies are needed that can preserve muscle mass, promote muscle growth, and maintain structure and function of both skeletal muscle and the myocardium without deleterious effects on the dystrophic heart.[28]

A contributing mechanism to the improved skeletal muscle pathology we observed in young dystrophic mice after Hsp72 induction was the preservation of maximal sarcoplasmic/endoplasmic reticulum Ca^{2+}-ATPase (SERCA) activity, the main protein responsible for removal of intracellular Ca^{2+} from the cytosol.[14] Because DMD is characterized by muscle fibers with chronically elevated intracellular Ca^{2+} ($[Ca^{2+}]_i$) levels that can activate inflammatory and muscle degradative pathways, and because SERCA dysfunction is implicated in the skeletal muscle and cardiac pathologies,[29,30] we also tested whether BGP-15 treatment preserved SERCA activity in the heart.[14,31,32]

Materials and Methods

Experimental Animals

All experiments were approved by the Animal Ethics Committee of The University of Melbourne (Melbourne, VIC, Australia) and conducted in accordance with the Australian code of practice for the care and use of animals for scientific purposes, as stipulated by the National Health and Medical Research Council (Australia). C57BL/10 mice were obtained from the Animal Resources Centre (Canning Vale, WA) and *dko* mice [originally provided through collaboration with Prof. Dame Kay Davies (University of Oxford, Oxford, UK)] were bred in the Biological Research Facility at The University of Melbourne.[33] Genotypes from tail biopsy specimens were determined using real-time PCR with specific probes designed for each gene (Transnetyx Inc., Cordova, TN). All experimental mice were male and were housed under a 12-hour light/dark cycle with food and standard chow provided ad libitum.

To assess whether BGP-15 administration could confer effects on an already established dystrophic pathology, 20-week-old *mdx* and 8-week-old *dko* mice were administered BGP-15 (15 mg/kg in 0.9% sterile saline; N-Gene Research Laboratories Inc., New York, NY) daily via oral gavage for 4 (*dko*) or 5 (*mdx*) weeks. Age-matched vehicle-treated dystrophic and healthy wild-type control (C57BL/10) mice received an equivalent volume of 0.9% sterile saline via daily oral gavage. Because of the severity of the *dko* phenotype, a shorter treatment period was used with a significant number of mice reaching humane end point criteria (ie, kyphosis score of 5 and sustained 15% loss of body mass) after 12 weeks of age. The average lifespan of mice in our *dko* colony was approximately 14 to 15 weeks, with the severity of the dystrophic pathology at 8 weeks of age (when treatment commenced) indicated by an average kyphosis score of 2.5. The kyphosis score indicates the severity of spinal curvature on palpation of conscious mice and ranked 1 to 5, with 1 indicating no spinal deformity and 5 being the most severe. To assess the effect of BGP-15 administration as a preventive treatment for the dystrophic cardiomyopathy and to confirm previous findings on skeletal muscles of young mice,[14] 4-week-old *dko* mice were administered BGP-15 (15 mg/kg in 0.9% sterile saline daily via oral gavage) for 5 to 6 weeks, with other groups of aged-matched *dko* and C57BL/10 mice treated similarly with vehicle only. Because BGP-15 is a hydroxylamine derivative that affects only stressed cells, a group of C57BL/10 mice treated with BGP-15 was not included.[10,14,34] Previous

studies investigating BGP-15 effects on skeletal muscle and heart observed no morphological or functional changes in either tissue, in wild-type mice after long-term treatment.[14,34] To assess Hsp72 induction via BGP-15, 4- and 10-week-old *dko* mice and age-matched C57BL/10 mice were administered a single bolus of BGP-15 (15 mg/kg) via oral gavage, and the tibialis anterior (TA) muscles, heart, and diaphragm were excised 6 hours later, frozen in liquid nitrogen, and stored at −80°C for later analyses.

To determine whether basal expression levels of Hsp72 might account for lack of significant induction in diaphragm muscle from *dko* mice, basal expression levels were examined in young and older adult C57BL/10, *mdx*, and *dko* mice. All young mice assessed were 4 weeks of age across all genotypes. The older adult C57BL/10 and *mdx* mice were 20 weeks of age, but the *dko* mice were assessed at 10 weeks of age because of their truncated lifespan.

Assessment of Skeletal Muscle Contractile Properties

At the conclusion of the treatment period, mice were anesthetized with sodium pentobarbital (Nembutal; 60 mg/kg; Sigma-Aldrich, Castle Hill, NSW, Australia) via i.p. injection and contractile properties of the mouse TA muscles assessed *in situ*, as described previously.[35] At the conclusion of these measurements, the TA, extensor digitorum longus, soleus, and quadriceps muscles were carefully excised, blotted on filter paper, and weighed on an analytical balance. The TA muscle was mounted in embedding medium and frozen in thawing isopentane for later histochemical analyses. TA muscle cross-sectional area was determined from the equation: Cross-Sectional Area = Muscle Mass/(L_f × 1.06), where L_f represents optimal fiber length and 1.06 represents the density of mammalian skeletal muscle.[36] The entire diaphragm and rib cage were surgically excised, and costal diaphragm muscle strips composed of longitudinally arranged full-length muscle fibers were isolated and prepared for functional assessment *in vitro*, as described previously.[37] On completion of the functional analyses, the diaphragm muscle strip was trimmed of tendon and any nonmuscle tissue, blotted once on filter paper, weighed on an analytical balance, mounted in embedding medium, and frozen in thawing isopentane for later histochemical analyses. Mice were sacrificed as a consequence of diaphragm and heart excision while anesthetized deeply. Hearts were trimmed of atria, the midsections removed and mounted in embedding medium, frozen in liquid nitrogen−cooled isopentane, and stored at −80°C for histochemical analyses. The remaining two-thirds of the ventricles were frozen in liquid nitrogen and stored at −80°C for subsequent biochemical analyses.

Echocardiographic Analysis of Cardiac Structure and Function

At the end of treatment, cardiac structure and function were evaluated by transthoracic two-dimensional B- and M-mode echocardiography (GE Vivid 9 15-mHz i13L linear array transducer; General Electric, Fairfield, CT) performed under light anesthesia (inhalation of isoflurane at 1.5%). Acquisition and offline analysis was performed with GE EchoPac software version 110, revision 1.8 (General Electric). The parasternal short axis was used for systolic parameters (interventricular septum, left ventricular posterior wall, left ventricular internal dimension, fractional shortening, ejection fraction, heart rate, stroke volume, end diastolic volume, and end systolic volume). Mitral valve (MV) blood flow Doppler (early filling MV E, active filling MV A) and tissue Doppler (early filling MV E′, active filling MV A') were measured in apical four-chamber view for diastolic parameters. For each measurement, at least three consecutive cycles were sampled. Because exercise can exacerbate the pathology in dystrophic mice,[38] mice used for cardiac analysis underwent voluntary wheel running (using Activity Wheel Monitor software model 86065; Lafayette Instruments, Lafayette, IN) overnight, either 48 or 72 hours before echocardiography. There were no differences in parameters between mice that were run 48 or 72 hours before analysis (data not shown).

Evans Blue Dye Uptake and Histology

To quantify cardiomyocyte damage and local areas of necrosis, Evans Blue Dye (Sigma, St. Louis, MO) was injected i.p. (1% w/v; 10 μL per gram body mass), as described previously,[14] and hearts excised and frozen 24 or 48 hours later. Sections (5 μm thick) were cut on a cryostat and Evans Blue Dye detected as red autofluorescence using a fluorescence microscope (Axio Imager D1; Carl Zeiss, Göttingen, Germany). There was no difference in Evans Blue Dye infiltration or echocardiographic parameters between mice injected at 24 or 48 hours before analysis (data not shown).

Serial sections (5 μm thick) were cut transversely through the TA, diaphragm, and heart using a refrigerated (−20°C) cryostat (CTI Cryostat; IEC, Needham Heights, MA) and stained with Masson trichrome or Van Gieson stain to assess collagen infiltration. Digital images were obtained using an upright microscope with camera (Axio Imager D1), controlled and quantified using AxioVision AC software release 4.8.2 (Carl Zeiss).

Antibodies

The following primary antibodies were used: Hsp70 (ADI-SPA-812; Enzo Life Sciences, Farmingdale, NY), SERCA1 ATPase (ab2812; Abcam, Cambridge, UK), SERCA2 ATPase (MA3-919; Thermo Fisher Scientific, Scoresby, VIC, Australia), Ser16 phospholamban (PLN; 07-052; Upstate, Lake Placid, NY), Thr17 PLN (AO10-13; Badrilla, Leeds, UK), total PLN (05-205; Upstate), cyclophilin F (D) (ab110324; Abcam), P-p65 (30335; Cell Signaling, Beverly, MA), T-p65 (47645; Cell Signaling), P-Jun N-terminal kinase (JNK) 1 and 2 (ab4821; Abcam), T-JNK 1 and 2

(Sc-7345; Santa Cruz Biotechnology, Dallas, TX), MitoProfile (MS604; MitoSciences, Eugene, OR), P-IGF-R1β (3024S; Cell Signaling), and total IGF-R1β (F0805; Santa Cruz Biotechnology). All primary antibodies were diluted in 5% bovine serum albumin/Tris-buffered saline−Tween-20 at 1:1000 [Hsp70, SERCA1 ATPase, SERCA2 ATPase, P- and T-p65, P- and T-JNK 1, cyclophilin D, MitoProfile, P-insulin-like growth factor-1β receptor (IGFR1β), and T-IGFR1β], 1:3000 (Ser16 PLN, total PLN), or 1:5000 (Thr17 PLN). It was necessary to use a positive control for the detection of phosphorylated IGFR, and C2C12 treated with insulin and anisomycin (Cell Signaling; 21101S) was used for this purpose.

Western Blotting

Skeletal muscles and hearts were immediately snap frozen in liquid nitrogen. Muscle samples (20 to 30 mg) were homogenized (Polytron 2100; Kinematica, Lucerne, Switzerland) for 3 to 15 seconds on ice in homogenizing buffer [10 mmol/L Tris-HCl, pH 7.5; 100 mmol/L sodium chloride; 1 mmol/L EDTA; 1 mmol/L EGTA; 10% glycerol; 1% Triton X-100; 0.1% SDS; 1 mmol/L sodium fluoride; 20 mmol/L sodium pyrophosphate; 2 mmol/L sodium orthovanadate; 0.5% sodium deoxycholate; 1 mmol/L phenylmethanesulphonylfluoride; 0.1% protease inhibitor cocktail (P8340; Sigma-Aldrich, Castle Hill, NSW, Australia); and 0.1% phosphatase inhibitor cocktail (P2850, P5726; Sigma-Aldrich)]. Homogenates were resolved in Laemmli buffer before heating to 95°C for 5 minutes and being separated by SDS-PAGE. Separated proteins were transferred to polyvinylidene difluoride membranes (0.45-mm Immobilon-P; Millipore, North Ryde, NSW, Australia). Membranes were blocked with 5% bovine serum albumin in Tris-buffered saline containing Tween-20 for 1 hour and incubated overnight at 4°C with antibody dilutions, as described previously (see *Antibodies*). Antibody binding was detected with horseradish peroxidase−conjugated immunoglobulin and visualized by chemiluminescent detection (ECL Prime Western Blotting detection reagent; Amersham, Amersham, UK) and imaging system (ChemiDoc XRS; Bio-Rad Laboratories, Hercules, CA). Band densities were quantified with Image Lab software version 4.1 (Bio-Rad Laboratories) and normalized to total protein content of the sample, as determined by BLOT-Fast Stain (G-Biosciences, St. Louis, MO).

SERCA Activity Assay

Maximal SERCA activity was assessed in whole muscle homogenates, as described previously.[14] Muscle samples (20 to 50 mg) were diluted in 200 μL of ice-cold homogenization buffer. Protease inhibitor cocktail (P2850, P5726; Sigma-Aldrich) was added immediately before use at a concentration of 5 μL per 100 mg of muscle tissue. Muscles were homogenized and centrifuged for 10 minutes at 5500 × *g* at 4°C, and supernatant was collected for SERCA activity analysis. Activity was determined in reaction buffer (200 mmol/L KCl, 20 mmol/L HEPES, pH 7.0, 15 mmol/L $MgCl_2$, 10 mmol/L NaN_3, 10 mmol/L phosphoenolpyruvate, 5 mmol/L ATP, and 1 mmol/L EGTA) with pH adjusted to 7.0 at 37°C. Immediately before starting the reaction, 18 U/mL pyruvate kinase, 18 U/mL lactate dehydrogenase, 5 μL NADH (100 mmol/L), 1 μmol/L calcimycin A-23187 (Sigma-Aldrich), and approximately 20 μL of whole muscle were added to 1 mL of reaction buffer in a plastic cuvette. Cuvettes were loaded into a spectrophotometer, and A_{340} was measured at 37°C (Multiscan Spectrum; Thermo Electron, Waltham, MA). Maximal SERCA activity was determined by progressively adding 100 mmol/L $CaCl_2$ until a plateau or maximal activity was reached. The specific SERCA inhibitor 29, 59-di(tert-butyl)-1, 4-benzohydroquinone, was added to a final concentration of 40 mmol/L to determine basal activity.

Superoxide Indicator Dihydroethidium Intensity

Fresh frozen heart cross sections (5 μm thick) were incubated in 2 μmol/L dihydroethidium (Life Technologies Australia, Scoresby, VIC) (0.1% dimethyl sulfoxide) in phosphate-buffered saline at 37°C for 30 minutes. Sections were rinsed in phosphate-buffered saline before air drying and application of cover with fluorescent mounting medium. Dihydroethidium intensity was detected as red fluorescence using a fluorescence microscope (Axio Imager D1).

Statistical Analysis

Data were analyzed with GraphPad Prism software version 7 (GraphPad Software Inc., La Jolla, CA). Unpaired *t*-tests were used for comparisons between two groups. For comparisons between more than two groups, a one- or two-way analysis of variance was used, as appropriate, with Tukey's post hoc multiple comparison test when significance was detected. The level of significance was set at $P < 0.05$ for all comparisons. All values are presented as means ± SEM.

Results

Later-Stage BGP-15 Treatment Does Not Improve Skeletal Muscle Pathology in Older *mdx* Mice

The *mdx* mouse is the most widely used animal model of DMD. To test the efficacy of later-stage treatment on the dystrophic muscle pathology, 20-week-old *mdx* mice were administered BGP-15 (15 mg/kg per day) via oral gavage for 5 weeks. Treatment did not change body mass or muscle mass normalized to body mass (Figure 1, A and B) and did not improve maximal force output or force output over a range of stimulation frequencies in either diaphragm muscle strips (*in vitro*) or TA muscles (*in situ*) (Figure 1, C−F). Fibrotic infiltration was not different in the diaphragm

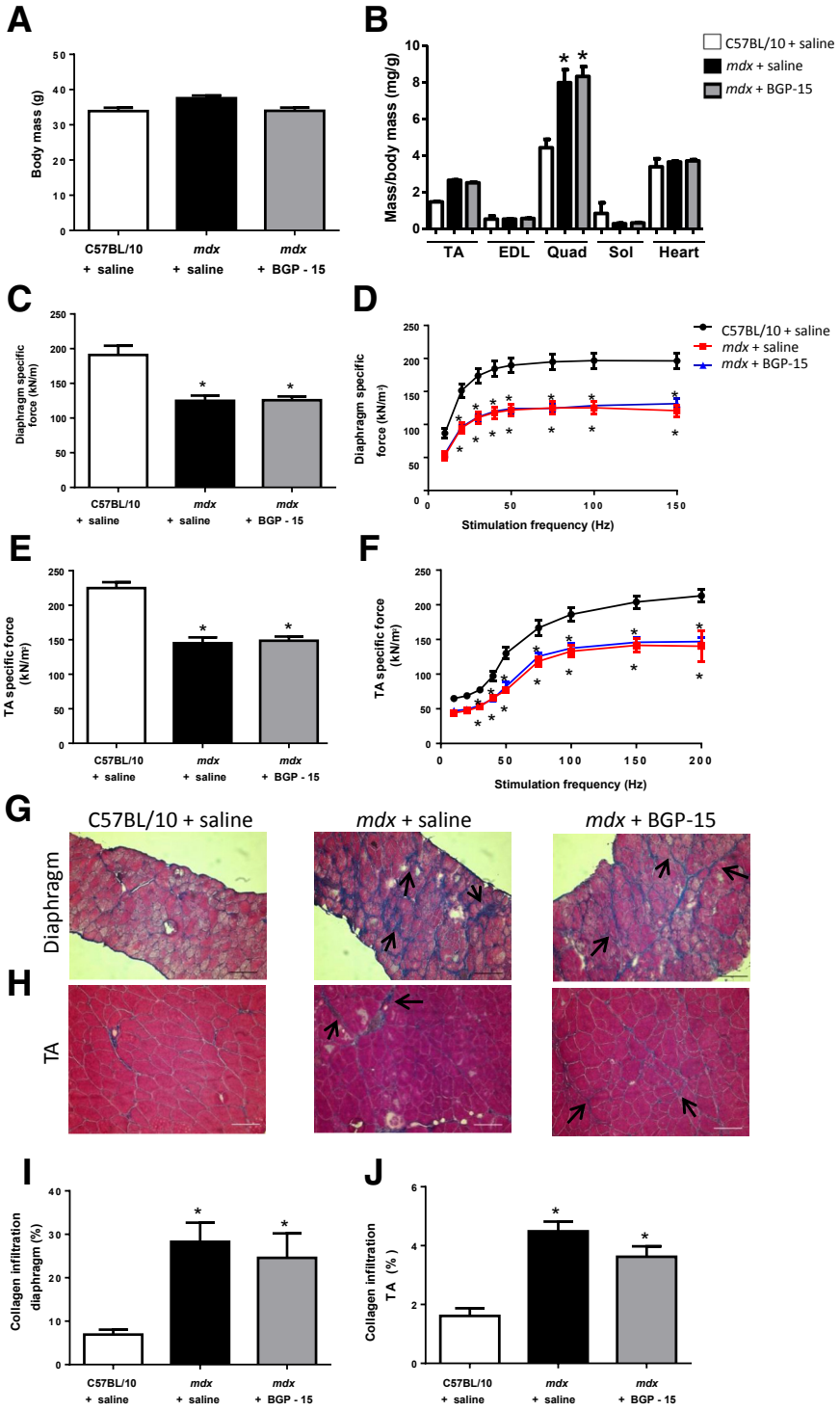

Figure 1 Body mass, muscle mass, contractile properties, and collagen infiltration of skeletal muscles of older *mdx* mice administered BGP-15 compared with saline-treated *mdx* and C57BL/10 control mice. Body mass (**A**) and muscle mass normalized to body mass (**B**) were unchanged with treatment. Peak specific force (**C**) and specific force over a range of stimulation frequencies of diaphragm muscle strips assessed *in vitro* (**D**); and peak specific force (**E**) and specific force over a range of stimulation frequencies for tibialis anterior (TA) muscles assessed *in situ* (**F**) were not improved with BGP-15 treatment. Representative images and quantification of collagen infiltration (blue, highlighted by **arrows**) in the diaphragm (**G** and **I**) and TA muscles (**H** and **J**) showed no change with BGP-15 treatment. $n = 11$ to 12 (**A** and **B**); $n = 10$ to 11 (**C** and **D**); $n = 10$ (**E** and **F**); $n = 7$ to 8 (**I**); $n = 5$ to 8 (**J**). $^*P < 0.05$ versus C57BL/10 + saline. Scale bars = 100 μm (**G** and **H**). Original magnification, ×126 (**G** and **H**). EDL, extensor digitorum longus; Quad, quadriceps; Sol, soleus.

(Figure 1, G and I) or TA muscles (Figure 1, H and J) of treated compared with untreated older *mdx* mice. Because the most significant pathological alterations occur in *mdx* mice between 2 and 8 weeks of age and the disease progresses relatively slowly until approximately 18 months of age,[39,40] the lack of an effect of BGP-15 treatment in older *mdx* mice is likely attributed to the lack of disease progression during this period.

BGP-15 Induces Hsp72 Expression in the TA Muscles and Heart But Not in the Diaphragm of *dko* Mice

The *dko* mouse, which lacks dystrophin and the homologous protein utrophin, exhibits a severe phenotype that more closely resembles the disease progression in DMD.[33,41] Although BGP-15 can induce Hsp72 in the diaphragm muscles of *mdx* mice,[14] its capacity to induce

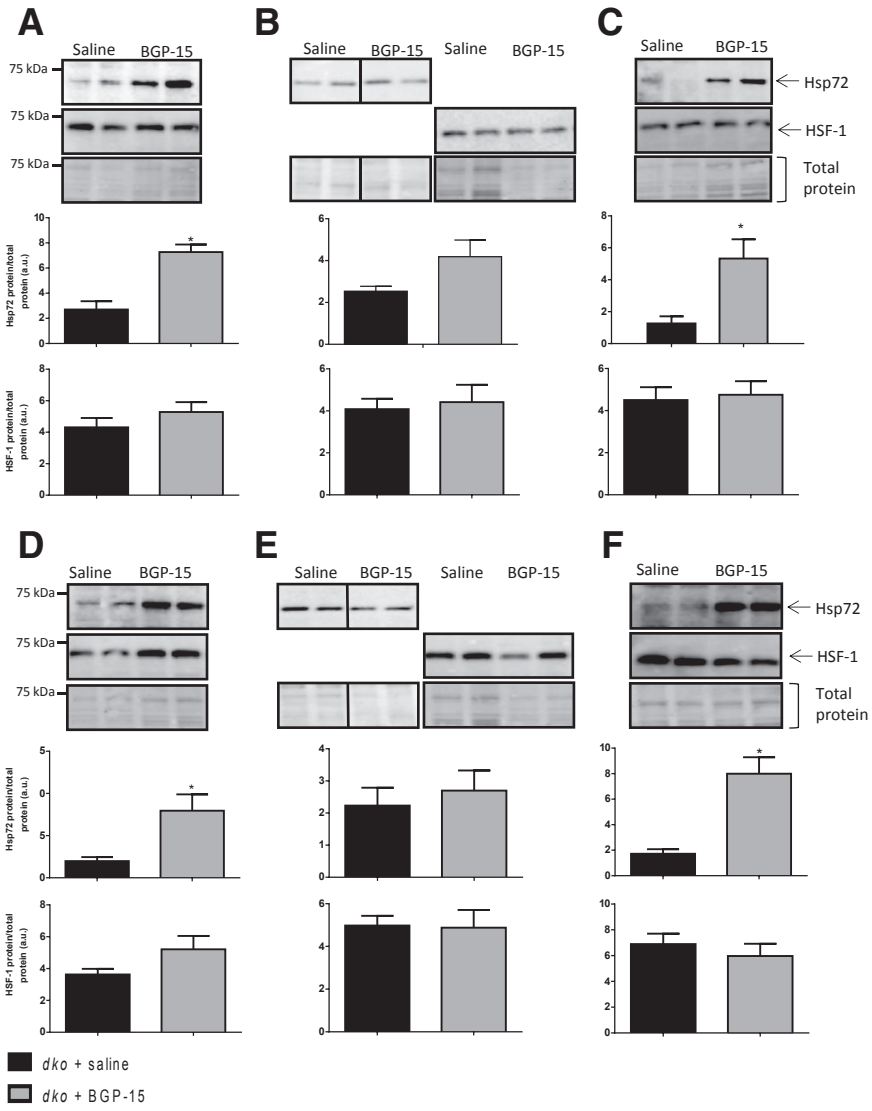

Figure 2 Induction of heat shock protein (Hsp) 72 and heat shock factor (HSF)-1 protein expression after a single bolus of saline (black bars) or BGP-15 (gray bars) in tibialis anterior (TA) muscles, diaphragm muscles, and the heart of 4-week-old (**A**–**C**) and 10-week-old (**D**–**F**) *dko* mice, respectively. Representative blots and quantification of Hsp72 (**top panels**) and HSF-1 (**bottom panels**) protein expression, normalized to total protein, 6 hours after a single bolus of saline (black bars) or BGP-15 (gray bars) in TA muscles (**A** and **D**), diaphragm muscles (**B** and **E**), and the heart (**C** and **F**) of 4- and 10-week-old *dko* mice, respectively. In **B** and **E**, representative western blots for Hsp72 and HSF-1 were performed on separate membranes and therefore corresponding total protein stains are shown. A **straight line** through representative membranes indicates where they have been spliced. $n = 8$ (**A**); $n = 6$ to 10 (**B**); $n = 7$ to 8 (**C**); $n = 8$ (**D** and **E**); $n = 6$ to 7 (**F**). $^*P < 0.05$ versus *dko* + saline. a.u., arbitrary unit.

Hsp72 expression in *dko* mice had not been determined. Because BGP-15 indirectly induces Hsp72 expression by activating heat shock factor 1 (HSF-1), the basal expression of which is reduced in other models of myopathy,[10] it is possible that Hsp72 induction could be diminished if the pathology is well progressed. The effect of BGP-15 on Hsp72 and HSF-1 protein expression was investigated in TA muscles (Figure 2, A and D), diaphragm (Figure 2, B and E), and hearts (Figure 2, C and F) of young 4-week-old *dko* mice and more severely affected 10-week-old *dko* mice. Muscles were excised 6 hours after administration of a single bolus of BGP-15 (15 mg/kg) or saline, which has previously been shown to be the optimal time point for Hsp72 induction.[42] No BGP-15–treated C57BL/10 mice were included because BGP-15 induces Hsp72 expression only in stressed cells and has no effect on otherwise healthy wild-type mice.[10,14,19,34] We verified this in 4- and 10-week-old C57BL/10 mice administered a single bolus of BGP-15 (15 mg/kg) or saline via oral gavage, where Western blot analysis revealed no induction of Hsp72 in TA muscles, diaphragm, or hearts of wild-type mice at either age after BGP-15 administration (Supplemental Figure S1).

Hsp72 expression was induced significantly in the TA muscles and hearts of 4- and 10-week-old *dko* mice (Figure 2, A, C, D, and F), but not in the diaphragm of 4- ($P = 0.1$) or 10- ($P = 0.98$) week-old *dko* mice (Figure 2, B and E). HSF-1 expression was not different between 4- and 10-week-old *dko* mice and not altered after BGP-15 treatment (Figure 2, A–F). Comparison of Hsp72 induction levels between 4- and 10-week-old mice revealed no differences in TA, diaphragm, and heart muscles from *dko* mice (Supplemental Figure S2). In addition, no differences were observed in HSF-1 protein expression between 4- and 10-week-old *dko* mice (Supplemental Figure S3).

The basal expression levels of HSF-1 and Hsp72 were also assessed to see if there was an impact on

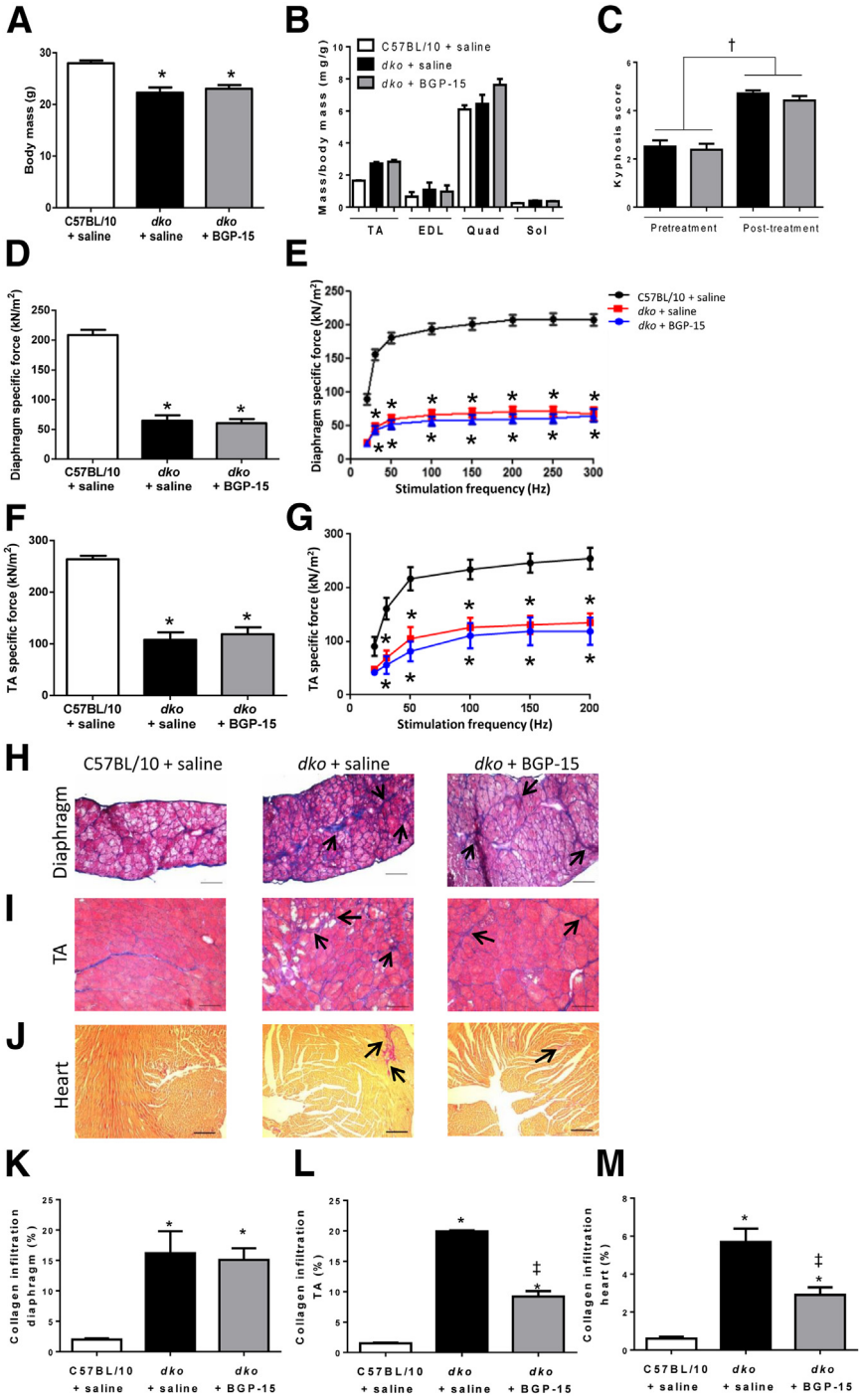

Figure 3 Body mass, muscle mass, kyphosis score, contractile properties, and collagen infiltration in skeletal muscles and hearts of older *dko* mice administered BGP-15 as a later-stage treatment compared with saline-treated *dko* and C57BL/10 control mice. Body mass (**A**), muscle mass normalized to body mass (**B**), and progression of kyphosis (**C**) were unchanged with treatment. Peak specific force and specific force over a range of stimulation frequencies of diaphragm muscle strips assessed *in vitro* (**D** and **E**) and tibialis anterior (TA) muscles assessed *in situ* (**F** and **G**) were not improved with BGP-15 treatment. Representative images and quantification of collagen infiltration (blue, highlighted by **arrows**) in the diaphragm (**H** and **K**) show no improvement with treatment, but cross sections of TA muscles (**I** and **L**) and ventricles (**J** and **M**) from BGP-15—treated dystrophic mice showed a significant reduction compared with *dko* control mice. $n = 10$ to 12 (**A**—**G**); $n = 8$ (**K**—**M**). $^{*}P < 0.05$ versus C57BL/10 + saline; $^{\dagger}P < 0.05$ between pretreatment and post-treatment; $^{\ddagger}P < 0.05$ versus *dko* + saline. Scale bars: 100 μm (**H**—**J**). Original magnification, ×126 (**H**—**J**). EDL, extensor digitorum longus; Quad, quadriceps; Sol, soleus.

BGP-15—mediated induction. Hsp72 protein expression was elevated in TA muscles from 10-week-old *dko* mice compared with C57BL/10 and *mdx* mice (Supplemental Figure S4A). HSF-1 protein expression was elevated in the TA muscles of 4-week-old *mdx* mice compared with 10-week-old *mdx* mice (Supplemental Figure S4B). No significant differences in Hsp72 or HSF-1 protein expression were observed between experimental groups in the diaphragm (Supplemental Figure S5, A and B). Hsp72 protein expression was elevated in the hearts of 4-week-old C57BL/10 and *mdx* mice compared with 10-week-old C57BL/10 and *mdx* mice, respectively (Supplemental Figure S6A). However, no significant differences in HSF-1 protein expression were observed between groups in the heart (Supplemental Figure S6B).

Later-Stage BGP-15 Treatment Reduces Fibrosis in TA Muscles of Older *dko* Mice

Daily BGP-15 treatment of young *dko* mice delayed progression of the dystrophic pathology in skeletal muscles.[14]

To determine the efficacy of BGP-15 in mice with established muscle pathology, 8-week-old *dko* mice were administered BGP-15 (15 mg/kg per day) via oral gavage for 4 weeks. This shorter treatment period (compared to 5 weeks in *mdx* mice) was used because the phenotype of *dko* mice is severe and a large number of mice meet the humane end point criteria (kyphosis score of 5 and sustained 15% loss of body mass) by 12 weeks of age. BGP-15 treatment did not alter body mass (Figure 3A), muscle mass (Figure 3B), or kyphosis score (Figure 3C) in older *dko* mice with the established dystrophic pathology. No differences in maximal force of diaphragm muscle strips (Figure 3, D and E) or TA muscles (Figure 3, F and G) were observed between treated and untreated older *dko* mice. Collagen infiltration in the diaphragm was not altered with treatment (Figure 3, H and K) but was approximately 50% lower in TA muscles of treated *dko* mice compared with untreated *dko* mice (Figure 3, I and L). Collagen infiltration in ventricular cross sections was also lower in BGP-15–treated *dko* mice compared with saline-treated *dko* mice (Figure 3, J and M). Together, these data indicate more limited beneficial effects of BGP-15 when administered to older dystrophic mice with established disease pathology.

Later-Stage BGP-15 Treatment Does Not Improve SERCA Function in Muscles of Older *dko* Mice

Preserved SERCA function contributed to the improved dystrophic muscle pathophysiology in young *mdx* mice receiving BGP-15 early in life.[14] We therefore investigated whether BGP-15 treatment to older *dko* mice affected SERCA1 and SERCA2 protein expression and maximal SERCA activity in diaphragm and TA muscles. In the diaphragm, SERCA1 but not SERCA2 protein expression was lower in saline-treated *dko* mice compared with C57BL/10 controls (Figure 4, A and C). However, BGP-15 treatment did not significantly alter SERCA1 or SERCA2 protein expression compared with C57BL/10 controls or saline-treated *dko* mice (Figure 4, A and C). Maximal SERCA activity was

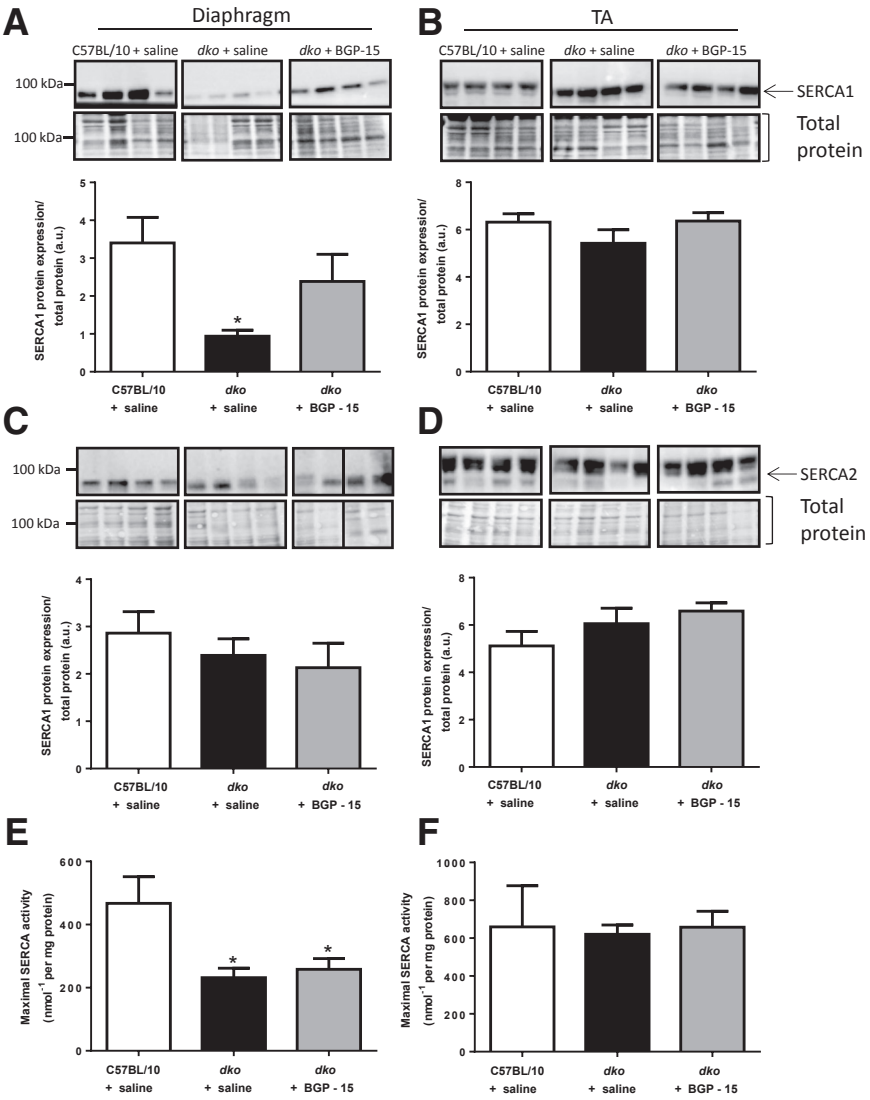

Figure 4 Sarcoplasmic/endoplasmic reticulum Ca^{2+}-ATPase (SERCA) protein expression and maximal activity in preparations from diaphragm and tibialis anterior (TA) muscles from older *dko* mice treated with BGP-15 as a later-stage treatment compared with saline-treated *dko* and C57BL/10 mice. Representative blots and quantification of SERCA1 protein expression in the diaphragm (**A**) and TA (**B**) muscles, SERCA2 protein expression in the diaphragm (**C**) and TA (**D**) muscles and maximal SERCA activity in the diaphragm (**E**) and TA (**F**) muscles from older BGP-15–treated *dko* mice compared with saline-treated *dko* and C57BL/10 mice. Protein expression was normalized to total protein expression. A **straight line** through representative membranes indicates where they have been spliced (**C**). $n = 8$ (**A**–**D**); $n = 10$ to 12 (**E** and **F**). *$P < 0.05$ versus C57BL/10. a.u., arbitrary unit.

decreased in diaphragm muscles from *dko* mice compared with C57BL/10 mice but was not improved with BGP-15 treatment (Figure 4E). In TA muscles, no differences in SERCA1 or SERCA2 protein expression or maximal SERCA activity were evident between groups (Figure 4, B, D, and F).

Early-Stage BGP-15 Treatment Improved Cardiac Pathology in Young *dko* Mice

In older *dko* mice, there was reduced collagen infiltration in ventricular cross sections in BGP-15–treated compared with untreated mice (Figure 3, J and M). Because BGP-15 induced the greatest improvements in skeletal muscle function when administered as an early intervention,[14] we also investigated whether treatment (15 mg/kg per day for 6 weeks) improved cardiac pathology in young 4-week-old *dko* mice. Because the phenotype of different *dko* mouse colonies can vary over time, we first confirmed the efficacy of BGP-15 to improve the skeletal muscle pathology in these mice. Consistent with our previous observations,[14] BGP-15–treated mice showed a significant reduction of collagen infiltration in the diaphragm (Supplemental Figure S7, A and B). Assessment of some hallmarks of the cardiac pathology revealed approximately 50% less collagen infiltration in ventricular cross sections of BGP-15–treated young *dko* mice (Figure 5, A and C). Increased permeability of the sarcolemma, as evident from Evans Blue Dye infiltration, was reduced by approximately 75% in the hearts of BGP-15–treated *dko* mice (Figure 5, B and D). These improvements occurred without any effect on heart mass normalized to tibial length (Figure 5E). Furthermore, tibial length did not vary between groups (C57BL/10 + saline, 12.86 ± 0.25 mm; *dko* + saline, 12.55 ± 0.12 mm; *dko* + BGP-15, 12.96 ± 0.19 mm; $P = 0.29$, $n = 8$ to 9).

Echocardiography at the end of the treatment period revealed left ventricular remodeling in the hearts of saline-treated *dko* mice (Figure 5F), with thinner posterior

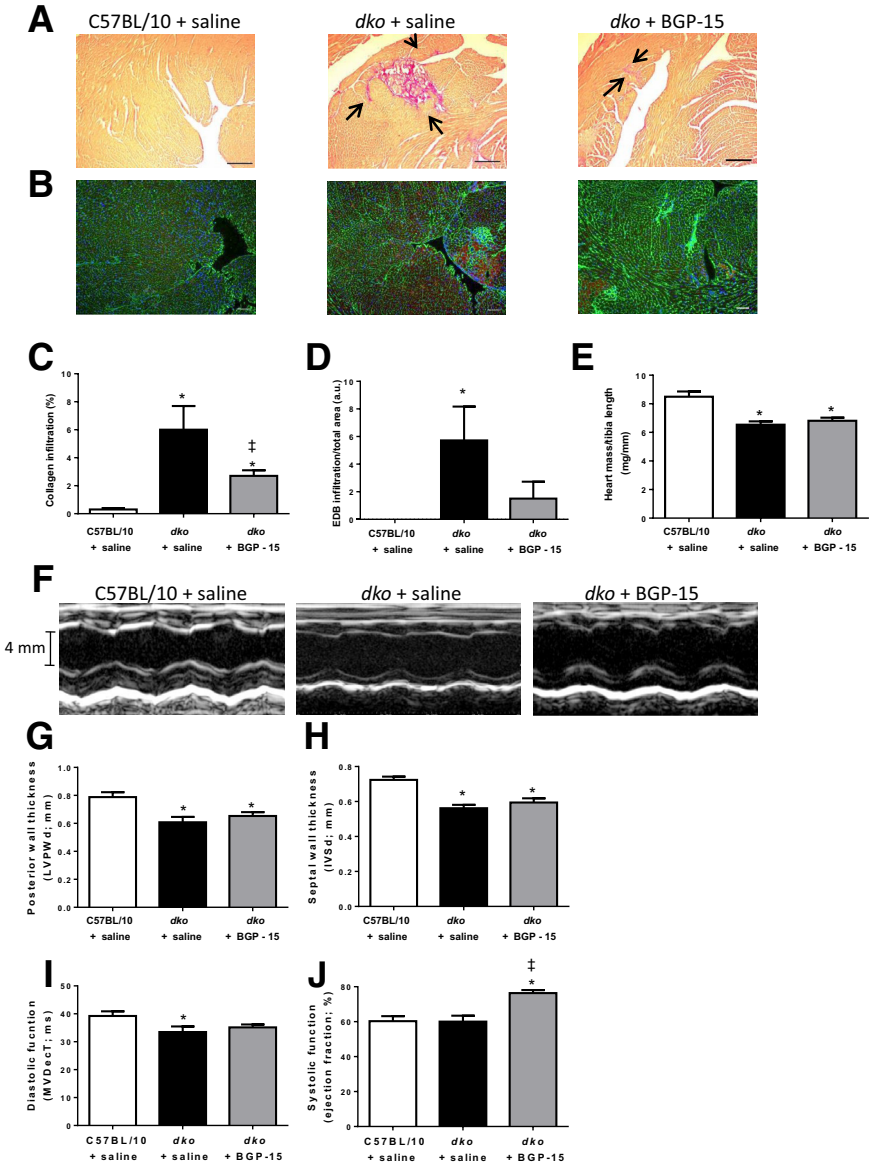

Figure 5 Collagen infiltration, membrane integrity, and echocardiographic analyses of the structure and function of hearts from young *dko* mice administered BGP-15 as an early-stage treatment compared with saline-treated *dko* and C57BL/10 control mice. Representative images of cardiac muscle cross sections stained with Van Gieson (**A**) and Evans Blue Dye (EBD; **B**) indicating collagen infiltration (pink, highlighted by **arrows**) and reductions in membrane integrity (red), respectively. Quantification of Van Gieson stain showing the percentage collagen infiltration in heart cross sections (**C**) and of EBD infiltration relative to total muscle area (**D**). **E:** Heart mass was normalized to tibial length. **F:** Representative images from M-mode echocardiogram showing interventricular septal wall, left ventricular (LV) posterior wall, and left ventricle chamber diameter during cardiac cycling. Quantification of posterior wall thickness (**G**) and septal wall thickness (**H**) at the end of diastole. **I:** Diastolic function was determined by deceleration time (MVDec T) of blood flow during early ventricular filling. **J:** Systolic function was represented by ejection fraction (%) assessed by B-mode echocardiogram. $n = 6$ to 8 (**C**–**E**); $n = 10$ to 12 (**G**–**J**). $^{*}P < 0.05$ versus C57BL/10 + saline; $^{‡}P < 0.05$ versus *dko* + saline. Scale bars: 100 μm (**A** and **B**). Original magnification: ×126 (**A**); ×63 (**B**).

Table 1 Echocardiographic Assessment of Left Ventricular Structure and Function of Young *dko* Mice Treated with BGP-15 as an Early-Stage Treatment Compared with Saline-Treated *dko* and C57BL/10 Control Mice

Variable	C57BL/10 + saline	*dko* + saline	*dko* + BGP-15
Geometry			
IVSd	0.72 ± 0.02	0.56 ± 0.02*	0.594 ± 0.02*
LVPWd	0.78 ± 0.04	0.60 ± 0.04*	0.653 ± 0.03*
LVIDd (mm)	3.9 ± 0.1	3.8 ± 0.1	3.7 ± 0.1
RWT	0.37 ± 0.02	0.31 ± 0.02	0.34 ± 0.02
Systolic function			
FS (%)	28 ± 2	28 ± 1	32 ± 1*
EF (%)	60 ± 3	60 ± 3	76 ± 2*
SV (μL)	96 ± 7	85 ± 7	86. ± 5
HR (bpm)	379 ± 17	414 ± 13	408 ± 15
EDV (μL)	30 ± 2	19 ± 2*	20 ± 1*
ESV (μL)	12 ± 5	8 ± 1	5 ± 1*
Diastolic function			
MV E (cm/second)	48.7 ± 1.4	47.3 ± 2.7	50.1 ± 2.9
MV A (cm/second)	24.3 ± 1.8	33.5 ± 2.7*	34.2 ± 2.3*
MV E/A	2.1 ± 0.1	1.5 ± 0.2*	1.5 ± 0.1*
MV E′ (mm/second)	2.2 ± 0.2	1.8 ± 0.2	2.3 ± 0.2
MV A′ (mm/second)	2.1 ± 0.2	2.2 ± 0.1	2.6 ± 0.2
MV E′/A′	1.2 ± 0.1	0.9 ± 0.1	0.9 ± 0.1
MV E/E′	21.9 ± 1.3	26.0 ± 2.3	22.7 ± 2.3

*$P < 0.05$ versus C57BL/10 + saline; $n = 10$ to 12.

EDV, end diastolic volume; EF, ejection fraction; ESV, end systolic volume; FS, fractional shortening; HR, heart rate; IVSd, interventricular septal thickness during diastole; LVIDd, left ventricular internal diameter during diastole; LVPWd, left ventricular posterior wall thickness during diastole; MV A or A′, active filling; MV E or E′, passive filling; RWT, relative wall thickness = [interventricular septal width + left ventricular posterior wall (d)]/LVIDd; SV, stroke volume.

(Figure 5G) and septal walls compared with C57BL/10 mice (Figure 5H). These parameters were not improved with BGP-15 treatment. Diastolic function was reduced significantly in saline-treated *dko* mice compared with C57BL/10 control mice (Figure 5I). Diastolic function of BGP-15–treated *dko* mice was not significantly different compared with saline-treated *dko* mice or C57BL/10 mice (Figure 5I). Systolic function was not different between saline-treated *dko* mice and C57BL/10 mice, but was 20% higher in BGP-15–treated *dko* mice (Figure 5J). No changes were observed in left ventricular chamber diameter between BGP-15–treated and saline-treated *dko* mice (Table 1). End diastolic volume was reduced in both *dko* groups, and end systolic volume was reduced only in the BGP-15–treated *dko* mice (Table 1). Active filling of the left ventricle, assessed by blood flow Doppler (MV A), was increased in both groups of *dko* mice (Table 1).

Early BGP-15 Treatment Does Not Alter SERCA Activity, Mitochondrial Proteins, or Inflammatory Markers in Hearts of Dystrophic Mice

To assess whether SERCA regulation contributes to the improved cardiac pathology in BGP-15–treated *dko* mice, SERCA2 protein expression and PLN phosphorylation were examined. PLN is a regulatory SERCA accessory protein that can be activated by phosphorylation at Ser16 and Thr17, and so both sites were assessed via Western blot and normalized to total PLN. Neither SERCA2 protein expression (Figure 6A) nor PLN phosphorylation at Ser16 (Figure 6B) or Thr17 (Figure 6C) was altered after BGP-15 treatment.

Previous studies identified mitochondrial dysfunction and JNK phosphorylation as potential mechanisms in myopathies other than muscular dystrophy.[10,11,14] We found no changes in phosphorylation of p65 (a component of the NF-κB inflammatory pathway) (Figure 6D), JNK (Figure 6, E and F), cyclophilin D (Figure 6G), superoxide indicator dihydroethidium (Figure 6H), or mitochondrial electron transport chain subunits (I-V) (Figure 6, I–M) in hearts from BGP-15–treated *dko* mice compared with untreated *dko* mice and C57BL/10 mice. However, some of these findings may be complicated by insufficient power. These parameters were also assessed in hearts from older *dko* mice treated with BGP-15, but no improvements were evident (Supplemental Figure S8).

BGP-15 Treatment Does Not Alter IGFR Phosphorylation in the Hearts of *dko* Mice

A recent study investigating the effect of BGP-15 on mice with an atrial fibrillation/heart failure phenotype showed improvements were independent of Hsp72 and corresponded with phosphorylation of the IGFR.[34] Phosphorylated IGFR and total IGFR were therefore assessed in hearts from young and old *dko* mice treated with BGP-15.

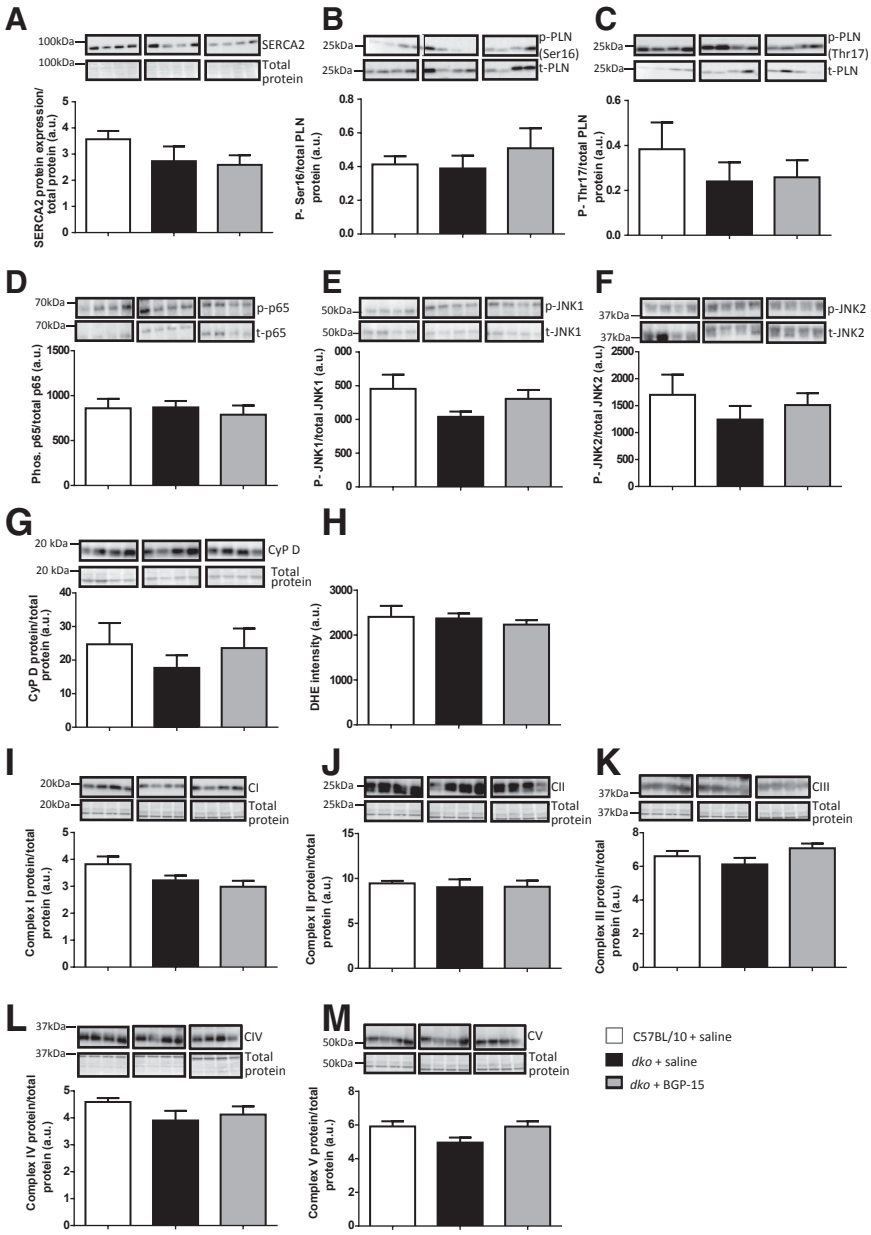

Figure 6 Sarcoplasmic/endoplasmic reticulum Ca^{2+}-ATPase (SERCA) 2 protein expression and phospholamban (PLN) Ser16 and Thr17 phosphorylation, inflammatory markers, and mitochondrial stress markers in hearts from young *dko* mice administered BGP-15 as an early-stage treatment. Representative blots and quantification of SERCA2 protein expression normalized to total protein (**A**), PLN Ser16 phosphorylation normalized to total PLN protein expression (**B**), and PLN Thr17 phosphorylation normalized to total PLN protein expression (**C**). Representative blots and quantification of phosphorylation of p65 (**D**), Jun N-terminal kinase (JNK) 1 (**E**), and JNK 2 (**F**) normalized to total values. Representative blots and quantification of cyclophilin D (CyP D) protein expression normalized to total protein (**G**) and quantification of the fluorescence intensity of dihydroethidium (DHE; **H**). **I**–**M:** Representative blots and quantification of mitochondrial electron transport chain subunits I to V protein (CI to CV) expression normalized to total protein. No significant differences were evident between groups. $n = 8$. a.u., arbitrary unit.

However, unlike this previous study, the phosphorylation levels detected via Western blot were too low for reproducible, quantifiable results. Phosphorylated and total IGFR were run on separate gels as the protein levels of IGFR did not allow for membrane stripping (Supplemental Figure S9, A and B). Although there were no apparent differences between groups, a contribution of IGFR phosphorylation remains possible.

Discussion

Consistent with our previous finding that BGP-15 improved the dystrophic pathology of skeletal muscles from young *mdx* and *dko* mice,[14] we confirmed that BGP-15 treatment of 4-week-old *dko* mice reduced skeletal muscle collagen infiltration and now reveal an improved cardiac pathology compared with untreated mice. Although BGP-15 treatment improved some aspects of the dystrophic pathology, such as fibrosis, it did not improve skeletal muscle function in older *mdx* or *dko* mice. Our findings identify a therapeutic window for BGP-15 treatment of muscular dystrophy in *dko* mice. For improvements in skeletal muscle parameters, BGP-15 should be administered as early as possible to slow the disease progression, whereas cardiac benefits were evident even when treating older mice. These results have therapeutic implications for when treatments should be administered clinically to different stages of the DMD pathology.

Although we had previously identified the therapeutic potential of Hsp72 induction and BGP-15 treatment for

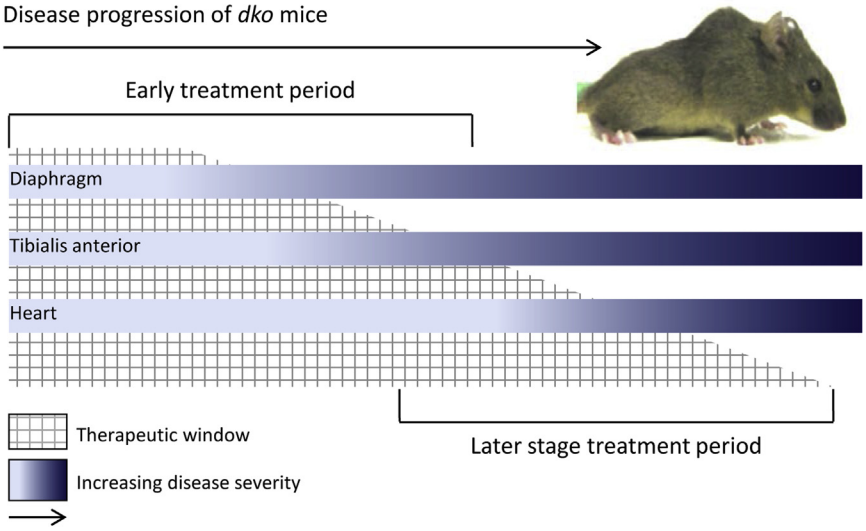

Figure 7 Proposed therapeutic window of opportunity for dystrophic mice. The increasing color intensity represents the severity of the progressive dystrophic pathology (derived from previous studies[33,41]), with the diaphragm being affected earlier and more severely than the tibialis anterior (TA) muscle or heart. The early and late treatments examined in this study are labeled to highlight the relative severity of the dystrophic pathology of each muscle during these periods. The therapeutic window for BGP-15 to potentially confer favorable effects (as determined from our studies) is represented by the hatched regions indicating the diaphragm and TA muscles have narrower therapeutic windows for BGP-15 to confer beneficial effects. The therapeutic window to potentially confer benefits to the heart is wider because the dystrophic cardiomyopathy progresses more slowly.

slowing the progression of the dystrophic pathology in the limb muscles and diaphragm of young *mdx* and *dko* mice,[14] these benefits of early treatment in dystrophic mice may not translate easily to the clinical setting given that DMD is not usually diagnosed until a significant muscle pathology is apparent. The lack of improvement in the skeletal muscle pathology of older *mdx* mice with BGP-15 treatment is not surprising. Given that the pathology is relatively stable at this age, and consistent with our previous findings showing that early- but not later-stage intervention with a myostatin inhibitory antibody improved the dystrophic pathology in *mdx* mice,[21] BGP-15 treatment is likely able to slow the disease progression but not reverse the pathology.

Basal expression levels of Hsp72 are higher in muscles of DMD patients and young *mdx* mice.[42,43] We assessed the basal expression of Hsp72 in the TA, diaphragm, and hearts of *dko* mice compared with C57BL/10 to determine whether this affected BGP-15–mediated induction. Although there were significant differences observed between groups, Hsp72 levels did not decrease with age and did not account for the pattern of Hsp72 induction observed after acute BGP-15 treatment. Therefore, differences in basal Hsp72 expression are unlikely to explain our observations that Hsp72 was not significantly induced in the diaphragm muscle after BGP-15 administration. It is possible that excessive collagen accumulation delays Hsp72 induction in the diaphragm muscle and we simply missed the increased expression because of the timing of sample collection (6 hours after BGP-15 administration). In addition, the lack of a clear relationship between changes in HSF-1 and HSP72 protein expression is not surprising as changes to HSF-1 expression occur earlier than with Hsp72.[10] Thus, the absence of altered HSF-1 and Hsp72 expression after BGP-15 treatment does not definitively refute this mechanism. Sapra et al[34] demonstrated phosphorylation of IGFR to be an alternative mechanism for BGP-15, improving cardiac function in mice with an atrial fibrillation/heart failure phenotype. We similarly assessed this mechanism but could not confirm phosphorylation of IGFR in the hearts of dystrophic mice after BGP-15 administration. If IGFR phosphorylation contributes to improvements in the hearts of *dko* mice, then its involvement is less apparent than in previous studies.[34]

We have shown that early-stage treatment of BGP-15 to more severely affected young *dko* mice reduced fibrosis in the diaphragm, increased lifespan, and improved skeletal muscle function.[14] Treating older *dko* mice with BGP-15 did not improve force-producing capacity of TA muscles and diaphragm muscle strips but reduced fibrosis in the TA muscles. Together, these data show reduced therapeutic efficacy of BGP-15 for dystrophic skeletal muscles when the disease is already well advanced. This is consistent with gene and pharmacological interventions that have had limited therapeutic efficacy as later-stage interventions.[21,44]

Although respiratory insufficiencies have previously accounted for approximately 90% of deaths in DMD, cardiomyopathy has become more prevalent and a critical aspect of the disease, presumably attributed to the increased use of corticosteroids and benefits of ventilator assist devices.[45] Because specific therapeutic targeting of the skeletal musculature (independent of the heart) can exacerbate the cardiomyopathy in *mdx* mice and prolonged ambulation in patients has been hypothesized to worsen the heart pathology,[46] targeting both skeletal and cardiac muscles is important so as to avoid accelerating the cardiac pathology. Our previous study[14] did not assess the effect of BGP-15 on the dystrophic heart, and because we observed the most pronounced improvements in the skeletal muscle pathology when mice were treated from a young age, we examined the effects of early-stage BGP-15 treatment on the hearts of young *dko* mice. BGP-15 reduced fibrosis, improved membrane integrity, and enhanced systolic function in *dko* mice. This is the second study to demonstrate the efficacy of

BGP-15 for cardiac pathologies, with Sapra et al[34] showing similarly beneficial effects in mice with an atrial fibrillation/heart failure phenotype. Although one study observed improved cardiac pathology with specific therapeutic targeting of skeletal muscle in dystrophic mice and hypothesized that improvements in diaphragm function could drive improvements in heart function,[47] it has also been shown that specific rescue of skeletal muscles in *mdx* mice induced cardiac dysfunction.[25] This effect is also observed in patients experiencing inherited X-linked dilated cardiomyopathy, where loss of dystrophin in the heart with little or no skeletal muscle pathology leads to an early-onset cardiac phenotype.[48] Therefore, if BGP-15 treatment was not exerting a direct effect on the heart, an exacerbation of cardiac pathology would be likely. Our observation of a clear and significant induction of Hsp72 in the hearts of *dko* mice means that BGP-15 treatment is having a direct effect on this tissue. As systolic function was not reduced in saline-treated *dko* mice relative to control, it was surprising to observe increased systolic function in the hearts of *dko* mice after BGP-15 administration. This effect is likely specific to the dystrophic condition because previous studies have shown no change in systolic function after BGP-15 administration to control mice.[34] We show herein that BGP-15 can improve aspects of the cardiac pathology and that treatment is not detrimental to the dystrophic heart. Although there is scope for the primary mechanism of cardiac improvement to derive from effects on the diaphragm or right ventricle,[47] our findings show that BGP-15 treatment can improve pathology in dystrophic hearts and has clinical merit for treating the cardiac pathology in DMD patients.

BGP-15 treatment has been shown to increase mitochondrial number and oxidative capacity and alter JNK signaling in other models of myopathy,[11] but we found mitochondrial dysfunction and inflammatory signaling were not different between dystrophic and wild-type mice and were unaltered with treatment. Despite BGP-15 having beneficial effects on the hearts of *dko* mice, the mechanisms underlying these improvements are unclear and further studies are required to elucidate these processes.

Based on findings from this study and our previous study,[14] we can conclude that in dystrophic mice, BGP-15 treatment improved diaphragm muscle pathology only when administered early in life and that the TA muscles and heart showed structural and functional benefits with early treatment, but also conferred structural improvements in older mice with a later-stage intervention. BGP-15's efficacy to improve the dystrophic pathology did not correlate with basal expression levels of Hsp72 in the muscles tested but was related to the stage when treatment commenced relative to the severity of disease, highlighting an optimal therapeutic window where each muscle can be targeted most effectively (Figure 7). A similar therapeutic window exists for antibody-mediated myostatin inhibition showing benefits in young *mdx* mice but not older mice,[21] and peptide-conjugated phosphorodiamidate morpholino oligomers—mediated exon skipping approaches being unable to prevent disease progression when administered to *dko* mice with an advanced pathology, despite a near complete restoration of dystrophin.[44] Clearly, different therapeutic approaches for DMD face similar limitations for optimal efficacy based on when treatment commences relative to the disease progression.

This notion is also supported by our finding that BGP-15 treatment in *dko* mice exerted muscle-specific effects. Previous analyses in *dko* mice revealed pathological features evident in the diaphragm within the first weeks of life and in TA muscles 3 to 4 weeks later, but effects in the heart were not observed until later in life.[33,41] An early intervention with BGP-15 improved the pathology in all muscles examined, whereas efficacy was diminished when treatment commenced later in older mice. The findings also suggest that muscles with a slower dystrophic progression (eg, the heart) can still benefit from a later intervention.

Fibrosis can be an irreversible feature of the DMD pathology[44,49] and is likely to be a major factor defining the therapeutic window for interventions like BGP-15. Fibrosis also impairs the efficacy of gene- and cell-based therapies by acting as a physical barrier for cell and viral delivery, replacing muscle fibers that could be targeted and restricting the spaces in which myofibers can regenerate.[6,50–52] Thus, early prevention of collagen infiltration, like with BGP-15, may improve treatment efficacy and expand the therapeutic window of opportunity for gene- and cell-based approaches when they eventually become viable for clinical implementation.

Although these findings support the efficacy of BGP-15 for treating the dystrophic pathology, further studies are required to clarify the mechanism by which these benefits occur to highlight alternative clinical applications for BGP-15 and clarify potential limitations. In addition, understanding how BGP-15 elicits different induction patterns of the Hsps across tissue types will help optimize its application. Our findings that BGP-15 can improve the cardiac pathology even in older *dko* mice help define the therapeutic window where it is likely to confer benefits for the different aspects of the dystrophic pathology and support its potential as a promising therapy for DMD.

Supplemental Data

Supplemental material for this article can be found at *http://dx.doi.org/10.1016/j.ajpath.2016.08.008*.

References

1. Emery AE: The muscular dystrophies. Lancet 2002, 359:687–695
2. Ervasti JM, Campbell KP: Membrane organization of the dystrophin-glycoprotein complex. Cell 1991, 66:1121–1131
3. Bushby K, Finkel R, Birnkrant DJ, Case LE, Clemens PR, Cripe L, Kaul A, Kinnett K, McDonald C, Pandya S, Poysky J, Shapiro F, Tomezsko J, Constantin C; DMD Care Considerations Working

Group: Diagnosis and management of Duchenne muscular dystrophy, part 2: implementation of multidisciplinary care. Lancet Neurol 2010, 9:177–189
4. Dubowitz V: Neuromuscular disorders in childhood: old dogmas, new concepts. Arch Dis Child 1975, 50:335–346
5. Jennekens FG, ten Kate LP, de Visser M, Wintzen AR: Diagnostic criteria for Duchenne and Becker muscular dystrophy and myotonic dystrophy. Neuromuscul Disord 1991, 1:389–391
6. Wilton SD, Fletcher S: Modification of pre-mRNA processing: application to dystrophin expression. Curr Opin Mol Ther 2006, 8: 130–135
7. Ellis RJ: The molecular chaperone concept. Semin Cell Biol 1990, 1: 1–9
8. Wyttenbach A, Carmichael J, Swartz J, Furlong RA, Narain Y, Rankin J, Rubinsztein DC: Effects of heat shock, heat shock protein 40 (HDJ-2), and proteasome inhibition on protein aggregation in cellular models of Huntington's disease. Proc Natl Acad Sci U S A 2000, 97:2898–2903
9. Cummings CJ, Mancini MA, Antalffy B, DeFranco DB, Orr HT, Zoghbi HY: Chaperone suppression of aggregation and altered subcellular proteasome localization imply protein misfolding in SCA1. Nat Genet 1998, 19:148–154
10. Chung J, Nguyen AK, Henstridge DC, Holmes AG, Chan MH, Mesa JL, Lancaster GI, Southgate RJ, Bruce CR, Duffy SJ, Horvath I, Mestril R, Watt MJ, Hooper PL, Kingwell BA, Vigh L, Hevener A, Febbraio MA: HSP72 protects against obesity-induced insulin resistance. Proc Natl Acad Sci U S A 2008, 105:1739–1744
11. Henstridge DC, Bruce CR, Drew BG, Tory K, Kolonics A, Estevez E, Chung J, Watson N, Gardner T, Lee-Young RS, Connor T, Watt MJ, Carpenter K, Hargreaves M, McGee SL, Hevener AL, Febbraio MA: Activating HSP72 in rodent skeletal muscle increases mitochondrial number and oxidative capacity and decreases insulin resistance. Diabetes 2014, 63:1881–1894
12. Senf SM, Howard TM, Ahn B, Ferreira LF, Judge AR: Loss of the inducible Hsp70 delays the inflammatory response to skeletal muscle injury and severely impairs muscle regeneration. PLoS One 2013, 8: e62687
13. McArdle F, Spiers S, Aldemir H, Vasilaki A, Beaver A, Iwanejko L, McArdle A, Jackson MJ: Preconditioning of skeletal muscle against contraction-induced damage: the role of adaptations to oxidants in mice. J Physiol 2004, 561:233–244
14. Gehrig SM, van der Poel C, Sayer TA, Schertzer JD, Henstridge DC, Church JE, Lamon S, Russell AP, Davies KE, Febbraio MA, Lynch GS: Hsp72 preserves muscle function and slows progression of severe muscular dystrophy. Nature 2012, 484:394–398
15. Literati-Nagy B, Peterfai E, Kulcsar E, Literati-Nagy Z, Buday B, Tory K, Mandl J, Sumegi B, Fleming A, Roth J, Koranyi L: Beneficial effect of the insulin sensitizer (HSP inducer) BGP-15 on olanzapine-induced metabolic disorders. Brain Res Bull 2010, 83:340–344
16. Literati-Nagy B, Kulcsar E, Literati-Nagy Z, Buday B, Peterfai E, Horvath T, Tory K, Kolonics A, Fleming A, Mandl J, Koranyi L: Improvement of insulin sensitivity by a novel drug, BGP-15, in insulin-resistant patients: a proof of concept randomized double-blind clinical trial. Horm Metab Res 2009, 41:374–380
17. Gombos I, Crul T, Piotto S, Gungor B, Torok Z, Balogh G, Peter M, Slotte JP, Campana F, Pilbat AM, Hunya A, Toth N, Literati-Nagy Z, Vigh L Jr, Glatz A, Brameshuber M, Schutz GJ, Hevener A, Febbraio MA, Horvath I, Vigh L: Membrane-lipid therapy in operation: the HSP co-inducer BGP-15 activates stress signal transduction pathways by remodeling plasma membrane rafts. PLoS One 2011, 6: e28818
18. Vigh L, Horvath I, Maresca B, Harwood JL: Can the stress protein response be controlled by "membrane-lipid therapy"? Trends Biochem Sci 2007, 32:357–363
19. Vigh L, Literati PN, Horvath I, Torok Z, Balogh G, Glatz A, Kovacs E, Boros I, Ferdinandy P, Farkas B, Jaszlits L, Jednakovits A, Koranyi L, Maresca B: Bimoclomol: a nontoxic, hydroxylamine derivative with stress protein-inducing activity and cytoprotective effects. Nat Med 1997, 3:1150–1154
20. Soti C, Nagy E, Giricz Z, Vigh L, Csermely P, Ferdinandy P: Heat shock proteins as emerging therapeutic targets. Br J Pharmacol 2005, 146:769–780
21. Murphy KT, Ryall JG, Snell SM, Nair L, Koopman R, Krasney PA, Ibebunjo C, Holden KS, Loria PM, Salatto CT, Lynch GS: Antibody-directed myostatin inhibition improves diaphragm pathology in young but not adult dystrophic mdx mice. Am J Pathol 2010, 176: 2425–2434
22. Burch M, Siddiqi SA, Celermajer DS, Scott C, Bull C, Deanfield JE: Dilated cardiomyopathy in children: determinants of outcome. Br Heart J 1994, 72:246–250
23. Ashford MW Jr, Liu W, Lin SJ, Abraszewski P, Caruthers SD, Connolly AM, Yu X, Wickline SA: Occult cardiac contractile dysfunction in dystrophin-deficient children revealed by cardiac magnetic resonance strain imaging. Circulation 2005, 112: 2462–2467
24. Eagle M, Bourke J, Bullock R, Gibson M, Mehta J, Giddings D, Straub V, Bushby K: Managing Duchenne muscular dystrophy: the additive effect of spinal surgery and home nocturnal ventilation in improving survival. Neuromuscul Disord 2007, 17: 470–475
25. Townsend D, Yasuda S, Li S, Chamberlain JS, Metzger JM: Emergent dilated cardiomyopathy caused by targeted repair of dystrophic skeletal muscle. Mol Ther 2008, 16:832–835
26. Ermolova NV, Martinez L, Vetrone SA, Jordan MC, Roos KP, Sweeney HL, Spencer MJ: Long-term administration of the TNF blocking drug Remicade (cV1q) to mdx mice reduces skeletal and cardiac muscle fibrosis, but negatively impacts cardiac function. Neuromuscul Disord 2014, 24:583–595
27. Chun JL, O'Brien R, Berry SE: Cardiac dysfunction and pathology in the dystrophin and utrophin-deficient mouse during development of dilated cardiomyopathy. Neuromuscul Disord 2012, 22:368–379
28. Lynch GS, Schertzer JD, Ryall JG: Therapeutic approaches for muscle wasting disorders. Pharmacol Ther 2007, 113:461–487
29. Rohman MS, Emoto N, Takeshima Y, Yokoyama M, Matsuo M: Decreased mAKAP, ryanodine receptor, and SERCA2a gene expression in mdx hearts. Biochem Biophys Res Commun 2003, 310: 228–235
30. Kim YK, Suarez J, Hu Y, McDonough PM, Boer C, Dix DJ, Dillmann WH: Deletion of the inducible 70-kDa heat shock protein genes in mice impairs cardiac contractile function and calcium handling associated with hypertrophy. Circulation 2006, 113:2589–2597
31. Blake DJ, Weir A, Newey SE, Davies KE: Function and genetics of dystrophin and dystrophin-related proteins in muscle. Physiol Rev 2002, 82:291–329
32. Mariol MC, Segalat L: Muscular degeneration in the absence of dystrophin is a calcium-dependent process. Curr Biol 2001, 11: 1691–1694
33. Deconinck AE, Rafael JA, Skinner JA, Brown SC, Potter AC, Metzinger L, Watt DJ, Dickson JG, Tinsley JM, Davies KE: Utrophin-dystrophin-deficient mice as a model for Duchenne muscular dystrophy. Cell 1997, 90:717–727
34. Sapra G, Tham YK, Cemerlang N, Matsumoto A, Kiriazis H, Bernardo BC, Henstridge DC, Ooi JY, Pretorius L, Boey EJ, Lim L, Sadoshima J, Meikle PJ, Mellet NA, Woodcock EA, Marasco S, Ueyama T, Du XJ, Febbraio MA, McMullen JR: The small-molecule BGP-15 protects against heart failure and atrial fibrillation in mice. Nat Commun 2014, 5:5705
35. Murphy KT, Chee A, Gleeson BG, Naim T, Swiderski K, Koopman R, Lynch GS: Antibody-directed myostatin inhibition enhances muscle mass and function in tumor-bearing mice. Am J Physiol Regul Integr Comp Physiol 2011, 301:R716–R726
36. Brooks SV, Faulkner JA: Contractile properties of skeletal muscles from young, adult and aged mice. J Physiol 1988, 404:71–82

37. Lynch GS, Rafael JA, Hinkle RT, Cole NM, Chamberlain JS, Faulkner JA: Contractile properties of diaphragm muscle segments from old mdx and old transgenic mdx mice. Am J Physiol 1997, 272: C2063–C2068
38. Grounds MD, Radley HG, Lynch GS, Nagaraju K, De Luca A: Towards developing standard operating procedures for pre-clinical testing in the mdx mouse model of Duchenne muscular dystrophy. Neurobiol Dis 2008, 31:1–19
39. Coulton GR, Curtin NA, Morgan JE, Partridge TA: The mdx mouse skeletal muscle myopathy, II: contractile properties. Neuropathol Appl Neurobiol 1988, 14:299–314
40. Lefaucheur JP, Pastoret C, Sebille A: Phenotype of dystrophinopathy in old mdx mice. Anat Rec 1995, 242:70–76
41. Grady RM, Teng H, Nichol MC, Cunningham JC, Wilkinson RS, Sanes JR: Skeletal and cardiac myopathies in mice lacking utrophin and dystrophin: a model for Duchenne muscular dystrophy. Cell 1997, 90:729–738
42. Carberry S, Zweyer M, Swandulla D, Ohlendieck K: Comparative proteomic analysis of the contractile-protein-depleted fraction from normal versus dystrophic skeletal muscle. Anal Biochem 2014, 446:108–115
43. Bornman L, Polla BS, Lotz BP, Gericke GS: Expression of heat-shock/stress proteins in Duchenne muscular dystrophy. Muscle Nerve 1995, 18:23–31
44. Wu B, Cloer C, Lu P, Milazi S, Shaban M, Shah SN, Marston-Poe L, Moulton HM, Lu QL: Exon skipping restores dystrophin expression, but fails to prevent disease progression in later stage dystrophic dko mice. Gene Ther 2014, 21:785–793
45. Eagle M, Baudouin SV, Chandler C, Giddings DR, Bullock R, Bushby K: Survival in Duchenne muscular dystrophy: improvements in life expectancy since 1967 and the impact of home nocturnal ventilation. Neuromuscul Disord 2002, 12:926–929
46. Colan SD: Evolving therapeutic strategies for dystrophinopathies: potential for conflict between cardiac and skeletal needs. Circulation 2005, 112:2756–2758
47. Crisp A, Yin H, Goyenvalle A, Betts C, Moulton HM, Seow Y, Babbs A, Merritt T, Saleh AF, Gait MJ, Stuckey DJ, Clarke K, Davies KE, Wood MJ: Diaphragm rescue alone prevents heart dysfunction in dystrophic mice. Hum Mol Genet 2011, 20:413–421
48. Berko BA, Swift M: X-linked dilated cardiomyopathy. N Engl J Med 1987, 316:1186–1191
49. Bostick B, Shin JH, Yue Y, Wasala NB, Lai Y, Duan D: AAV micro-dystrophin gene therapy alleviates stress-induced cardiac death but not myocardial fibrosis in >21-m-old mdx mice, an end-stage model of Duchenne muscular dystrophy cardiomyopathy. J Mol Cell Cardiol 2012, 53:217–222
50. Zhou L, Lu H: Targeting fibrosis in Duchenne muscular dystrophy. J Neuropathol Exp Neurol 2010, 69:771–776
51. Cordier L, Hack AA, Scott MO, Barton-Davis ER, Gao G, Wilson JM, McNally EM, Sweeney HL: Rescue of skeletal muscles of gamma-sarcoglycan-deficient mice with adeno-associated virus-mediated gene transfer. Mol Ther 2000, 1:119–129
52. Gargioli C, Coletta M, De Grandis F, Cannata SM, Cossu G: PlGF-MMP-9-expressing cells restore microcirculation and efficacy of cell therapy in aged dystrophic muscle. Nat Med 2008, 14:973–978